Pedestrian-Aware Supervisory Control System Interactive Optimization of Connected Hybrid Electric Vehicles via Fuzzy Adaptive Cost Map and Bees Algorithm

Ji Li, *Member, IEEE*, Yingqi Gu, *Member, IEEE*, Chongming Wang, Mingming Liu, *Member, IEEE*, Quan Zhou, *Member, IEEE*, Guoxiang Lu, Duc Truong Pham, and Hongming Xu

***Abstract*—Electrified vehicles are increasingly being seen as a means of mitigating the pressing concerns of traffic-related pollution. Due to the nature of engine-assisted vehicle exhaust systems, pedestrians in close proximity to these vehicles may experience events where specific emission concentrations are high enough to cause health effects. To minimize pedestrians' exposure to vehicle emissions and pollutants nearby, we present a pedestrian-aware supervisory control system for connected hybrid electric vehicles by proposing an interactive optimization methodology. This optimization methodology combines a novel fuzzy adaptive cost map and the Bees Algorithm to optimize power-split control parameters. It enables the self-regulation of inter-objective weights of fuel and exhaust emissions based on the real-time pedestrian density information during the optimization process. The evaluation of the vehicle performance by using the proposed methodology is conducted on the realistic trip map involving pedestrian density information collected from the University College Dublin campus. Moreover, two bootstrap sampling techniques and effect of communication quality are both investigated in order to examine the robustness of the improved vehicle system. The results demonstrate that 14.42% mass of exhaust emissions can be reduced for the involved pedestrians, by using the developed fuzzy adaptive cost map.**

***Index Terms*—Bees Algorithm; fuzzy reasoning; connected hybrid electric vehicles; interactive optimization; pedestrian-aware supervisory control system**

I. Introduction

NOWADAYS, transport-related air pollution is becoming a significant societal issue. In fact, road transport has not only contributed to various harmful health effects to citizens in cities, but also it has become the main factor to the global warming [1]–[3]. Consequently, new traffic solutions must be sought to effectively address such a challenge for sustainable societal benefits. In this context, plug-in hybrid electric vehicles (PHEVs) are increasingly seen as an efficient means of transportation in mitigating the growing air quality concerns of exhaust gas emissions from traditional internal combustion engines (ICE) [4]. Compared to a pure electric vehicle, a PHEV normally has more mileage, and more flexibility in the control of emission actuation [5], namely a driver is allowed to either switch to a full electric mode when the underlying environmental concern is most significant, e.g., a green zone/district in a city, or to the polluting mode when the resulting emissions have less effect [6].

Heuristic supervisory control systems have been favored by industry due to easy implementation and strong robustness. The rules are designed in accordance with intuition, human expertise, and/or mathematical models and, usually, without knowing driving information a priori [7]. For PHEVs, charge-depleting (CD) mode and charge-sustaining (CS) mode [8] are widely used that enable to maximize the usage of electricity at sufficient charge and maintain a safe state of charge at insufficient charge [9]. To reduce the development workload for energy management controllers, Quan et al. research a transferable representation modelling routine, where two artificial intelligence technologies of deep neural network [10] and Gaussian process regression [11] are developed to cooperate with an adaptive neuro-fuzzy inference system for knowledge transfer of the energy management controller. To maximize effectiveness of heuristic control strategies, global optimization approaches have been applied to optimize their parameters. Montazeri-Gh et al. firstly used the genetic algorithm (GA) to optimize control parameters of electric assist control strategy [12], in which global optimal solutions were obtained for pre-defined driving cycles. Particle swarm optimization (PSO) with easy implementation and the lower computational burden is widely used in the design and control optimization problems [13], [14]. However, when dealing with complex nonlinear problems e.g., HEV energy management, Pham et al. have proved that the original version of this algorithm often falls into a local optimum compared to other nature-inspired evolutionary algorithms [15].

Since HEV energy management is a continuous optimization problem, the definition of cost functions is strongly related to the driving conditions [16]. Due to the past isolated environmental information, a large number of researchers only focus on benefit of vehicle owners so treat sub-objective weights in the cost function simply as to be stationary, such as defined in [17], [18]. Considering the diversity of realistic

This work was supported by the BYD Auto Ltd, Shenzhen City, China. Grant No.: 1001636. (*Corresponding author: Guoxiang Lu and Hongming Xu)*

Ji Li, Quan Zhou, Duc Troung Pham, and Hongming Xu are with the Department of Mechanical Engineering, the University of Birmingham, Birmingham, U.K. (e-mail: j.li.1@bham.ac.uk; q.zhou@pgr.bham.ac.uk; d.t.pham@bham.ac.uk; h.m.xu@bham.ac.uk). Yingqi Gu is with the School of Computing, the Dublin City University, Dublin, Ireland. (e-mail: yingqi.gu@dcu.ie). Mingming Liu is with the School of Electronic Engineering, the Dublin City University, Dublin, Ireland. (e-mail: mingming.liu@dcu.ie). Chongming Wang is with Institute for Future Transport and Cities, Coventry University, Coventry, U.K. (ac8174@coventry.ac.uk). Guoxiang Liu is, Department of New Technology Development, BYD Company Limited, Shenzhen City, China. (lu.guoxiang@byd.com).

driving scenarios, dynamic cost functions may more precisely reflect the fitness of the holistic objects but need to be investigated. Most recently, the authors developed a system-level vehicle management strategy for a PHEV with response to the density of pedestrians across various routes [19]. This management system would benefit those most harmed by automotive emissions; namely, pedestrians. This contrasts with traditional vehicle management strategy which benefits the vehicle owners. But the problem is, as similar in [20], such a routing problem is extremely difficult to fully release the advantages of hybrid vehicles only by switching traction modes.

More recently, the significance of considering the connected and automated vehicle (CAV) technology for co-optimization of energy and emissions has been acknowledged [21]. In the work of Huang et al. [22], a predictive speed controller is presented for a CAV with both energy and emissions concern, where energy saving performance is dependent on the level of data sharing and constraint in NOx emission. Shao et al. develop a CAV control strategy to simultaneously optimize vehicle speed and transmission gear position under a vehicle platooning scenario [23]. By experimented validation, 10.6% of improvement in fuel efficiency has been achieved compared to the immediately preceding vehicle. Different connectivity mechanisms have been investigated by Vahidi et al. [24] that lead to energy saving potentials of CAVs, and the ways preview information can be used intelligently. However, communication issues, such as time delays, quantization errors, and packet loss pose a significant challenge to vehicle distributed control [25] even driving safety [26]. Up to now, few noticeable works have been documented within the context of EMSs for CAVs considering communication issues.

This paper aims to minimize pedestrians' exposure to vehicle emissions and pollutants nearby so that an interactive optimization methodology is proposed for the pedestrian-aware supervisory control system of connected PHEVs. Instead of considering the optimization of a PHEV pollution at a system level, our setting is to explicitly consider the detailed powertrain, whilst taking account of the pedestrian density information. With an addition of external pedestrian information and dynamic optimization objectives, optimization of the pedestrian-aware supervisory control system will become more difficult. As an advanced nature-inspired metaheuristic algorithm, Bees Algorithm (BA) takes an advantage of searching accurately narrow valleys and holes, and for highly multi-modal functions, which is expected to solve this new problem. This optimization methodology merges a new fuzzy adaptive cost map and BA to optimize power-split control parameters. Such treatment allows to self-regulate inter-objective weights of fuel and emissions based on real-time information of pedestrian density during the optimization process. Four main contributions of this paper include:

1) The architectures of the studied series-parallel hybrid powertrain and supervisory control system are analyzed, and the corresponding emission-oriented optimization problem is delivered.
2) By making use of the fuzzy satisfying approach, a fuzzy adaptive cost map is designed to represent the relationship between pedestrian density and the weights of cost maps.
3) The power-split control parameters are optimized by leveraging the BA based on the developed fuzzy adaptive cost map via pedestrian density information.
4) The cost map adaptability, interactive optimization performance, vehicle system robustness, and effect of communication quality are evaluated, respectively.

The rest of this paper is organized as follows: the scientific problem to be studied in this paper is formulated by modelling a PHEV in section II. The mechanism of the pedestrian-aware supervisory control system and the proposed interactive optimization methodology is described in section III. Section IV sets out the real-world driving cycle collection and learning sample expansion that were used in this paper. Section V discusses the results of 1). adaptability and optimization performance of the cost map; and 2). the vehicle system robustness. Conclusions are summarized in section VI.

II. Problem Statement

A. Vehicle Configuration

The series-parallel PHEV powertrain supervised by the vehicle controller, which includes one gasoline engine, one integrated starter-generator (ISG), one trans-motor and two energy sources of fuel and electricity as shown in Fig.1.

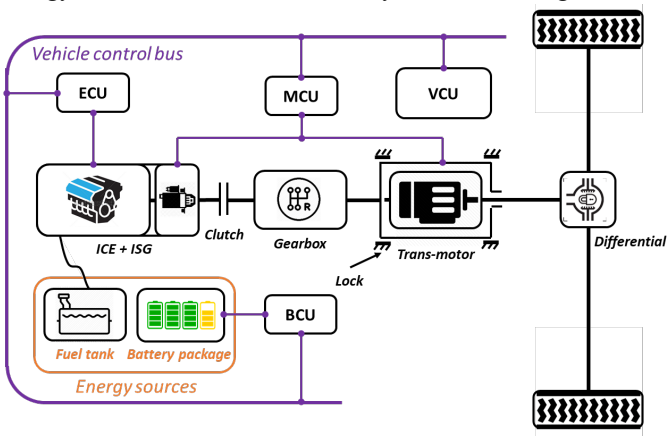

Fig.1. The structure of the series-parallel hybrid powertrain

In this case, the powers from the ICE after the transmission and the trans-motor are combined by coupling their speeds, where the speeds of the two power plants are decoupled to be chosen freely as described in [27]. The peak power of the trans-motor is $P_{mot^*} = 75$ kW (kilowatt) with 270 N · m (newton - meter) peak torque. The peak power of the gasoline engine is $P_{ICE^*} = 63$ kW with 140 N · m peak torque. The peak power of the ISG is $P_{ISG^*} = 32$ kW. The vehicle data, demonstrating a medium passenger car, was sourced from the authors' previous work [28] and their suitability has been established, where a 2RC electrical model [29] has been adopted to formulate a battery pack which consists of the battery cell type NCR-18650 series supplied by Panasonic Automotive & Industrial System Ltd. Table I shows the main parameters of the specific PHEV model.

TABLE I
MAIN PARAMETERS OF THE PHEV MODEL

Symbol	Parameters	Values
M	Gross mass	1,500 kg
A_f	Windward area	2 m^2
R_{wh}	Tire rolling radius	0.3 m
C_d	Air drag coefficient	0.3
i_0	Differential ratio	3.75
i_g	Gearbox ratio	3.55/1.96/1.30/0.89/0.71

The vehicle backward model with longitudinal dynamics is considered in this study, and the demand torque T_d and speed n_d after a bevel-gear speed reducer are:

$$\left.\begin{aligned} T_d &= \left(\delta ma + \frac{C_d A_f u^2}{21.15} + mgsin\theta + mgfcos\theta\right)\cdot\frac{R_{wh}}{i_0\cdot\eta_{i0}} \\ n_d &= \frac{P_d}{T_d} \end{aligned}\right\} \quad (1)$$

where, $g = 9.81 m/s^2$ is gravitational constant; $\delta = 1$ is the coefficient of rolling friction; $\theta = 0$ is slope grade; P_d is the demand power. The speeds of the ICE after transmission and the traction motor can be calculated via speed decoupling, which is expressed as

$$n_{mot} + n'_{ice} = n_d \quad (2)$$

in which

$$\begin{cases} n_{ice} = n'_{ice}\cdot i_g \\ T_{ice} = T_d \cdot i_g \end{cases} \quad (3)$$

where n_{ice} and n'_{ice} indicate rotation speeds of the ICE before and after transmission; T_{ice} indicates the demand torque of the ICE before transmission.

The transmission model uses a standard five-speed automatic gearbox to connect to the back end of the trans-motor; it provides the ICE with a proper gear ratio to achieve efficient operation. In order to avoid the case where a vehicle shifts up, the RPM is reduced in the new gear, then the vehicle shifts back down, starting an infinite up and downshifting situation, the shifting strategy adds supplementary constraints to the vehicle speed and acceleration, which ensure that a higher ratio always has priority when the gear ratio has more choices. Therefore, a gear ratio can be given:

$$i_g = \max\left(s_a(a_t), s_v(v_t)\right) \quad (4)$$

where i_g indicates output of the gear ratio; s_a and s_v are look-up tables used to find the corresponding gear ratios; and a_t and v_t are vehicle speed and acceleration. The shifting maps are drawn as:

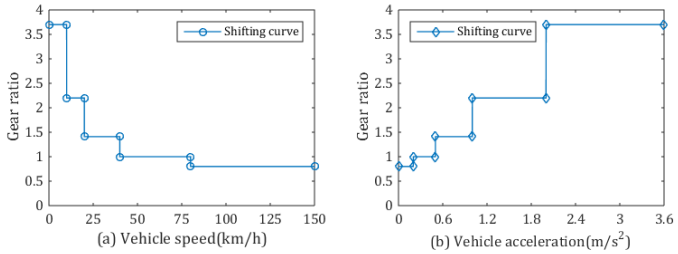

Fig.2. Shifting maps used in the research corresponding to: a) speed; and b) acceleration

B. Supervisory Control System

Given the hybrid configuration of this vehicle, a typical series-parallel state machine as illustrated in Fig.3 is adopted [30] to wisely arrange the usage of fuel and electricity based on the states of demand torque T_d, demand speed n_d, and battery pack's state of charge (SoC) SoC.

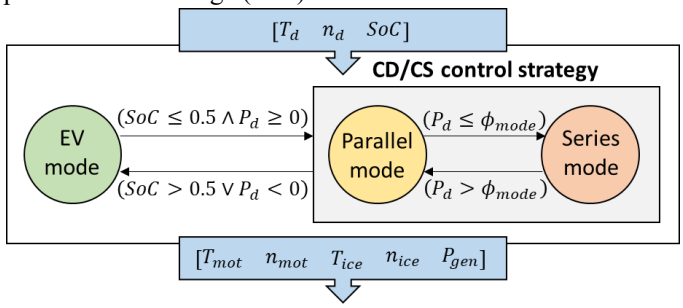

Fig.3. Overview of states of mode transition state machine

Here, a power-split vector $\boldsymbol{\xi}$ is constructed in Eq. (5), including the trans-motor torque, T_{mot}; the trans-motor speed, n_{mot}; the ICE torque, T_{ice}; the ICE speed, n_{ice}; the ISG power, P_{gen}.

$$\boldsymbol{\xi} = [T_{mot} \quad n_{mot} \quad T_{ice} \quad n_{ice} \quad P_{gen}] \quad (5)$$

In the EV mode (when $SoC \le 0.5 \wedge P_d \ge 0$), sufficient electricity can be provided to satisfy power demand of the PHEV independently thus both the ICE and the ISG can be idle in this case. The power allocation under the EV mode is described as follows:

$$\boldsymbol{\xi}_{EV} = [T_d \quad n_d \quad 0 \quad 0 \quad 0] \quad (6)$$

In the series and parallel modes (when $SoC > 0.5 \vee P_d < 0$), switching between series and parallel modes are governed by the demand power P_d and a control parameter ϕ_{mode}. If $P_d > \phi_{mode}$ the vehicle will work on parallel mode otherwise the vehicle will work on series mode. The control outputs for series mode and parallel mode are:

$$\left.\begin{aligned} \boldsymbol{\xi}_{series} &= [T_d \quad n_d\cdot(1-\chi_1) \quad T_d \quad n_d\cdot\chi_1 \quad 0] \\ \boldsymbol{\xi}_{parallel} &= [T_d \quad n_d \quad T'_{ice}(P_{gen}) \quad n'_{ice}(P_{gen}) \quad P^*_{gen}\cdot\chi_2] \end{aligned}\right\} \quad (7)$$

where, T'_{ice} and n'_{ice} are optimal torque and speed of the ICE converted based on demand power of the ISG P_{gen}; P^*_{gen} is the maximum power of the ISG; χ_i (i=1 or 2) is a proportionality factor determined by SoC as follows, χ_1 and χ_2 are for ICE control and ISG control, respectively [31].

$$\chi_i(SoC) = \begin{cases} 1, & SoC \in [0,0.2] \\ \left\{1+\exp\left[\left(\frac{SoC}{SoC^*}+\phi_{i,\beta}\right)\phi_{i,\alpha}\right]\right\}^{-1}, & SoC \in (0.2,0.5] \\ 0, & SoC \in (0.5,1] \end{cases} \quad (8)$$

where, SoC^* is a scaling coefficient of the BP's SoC; and $\phi_{i,\alpha}$ $(i = 1,2) \in [0.01,50]$ and $\phi_{i,\beta}(i = 1,2) \in [-6,6]$ are four control parameters for ICE and ISG.

III. PROPOSED SOLUTION

In order to minimize pedestrians' exposure to the vehicle emissions and fuel consumption and pollutants nearby, the interactive optimization methodology is proposed for the development of pedestrian-aware supervisory control system as illustrated in Fig.4. This optimization methodology we proposed combines a novel fuzzy adaptive cost map and the BA to optimize power-split control parameters. The design procedure includes three main phases: 1). conducting the

standardization and aggregation of cost maps of fuel, carbon monoxide (CO), hydrocarbon (HC), and nitrogen oxides (NOx); 2). reasoning the relationship between pedestrian density and weights of cost maps by using fuzzy satisfying approach; and 3). optimizing power-split control parameters via BA and the developed fuzzy adaptive cost map.

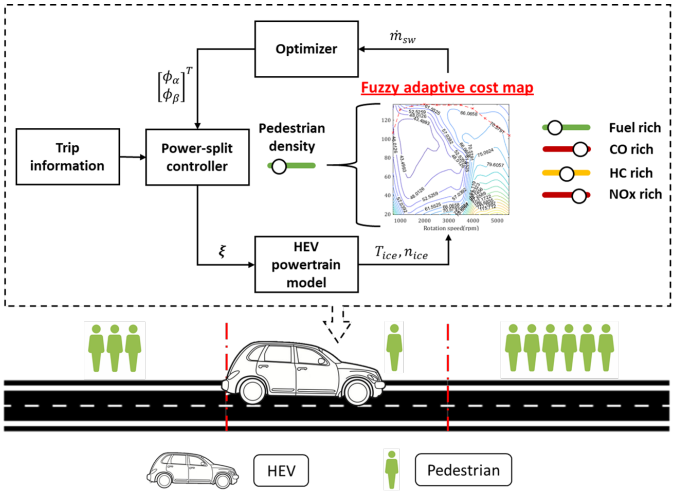

Fig.4. Schematic diagram of interactive optimization for the pedestrian-aware supervisory control system

A. Standardization of Cost Maps

Firstly, the standardization and aggregation for the exhaust emissions and fuel cost maps of the ICE is launched prior to achieving the self-adaptation to pedestrian density. The common approach that is taken in previous studies [32], [33] is to derive cost maps for fuel and the emission component in individual, then perform multi-objective optimization. This treatment combines multiple fuel and emission components into a single target for reducing computational burden from several table lookup operations.

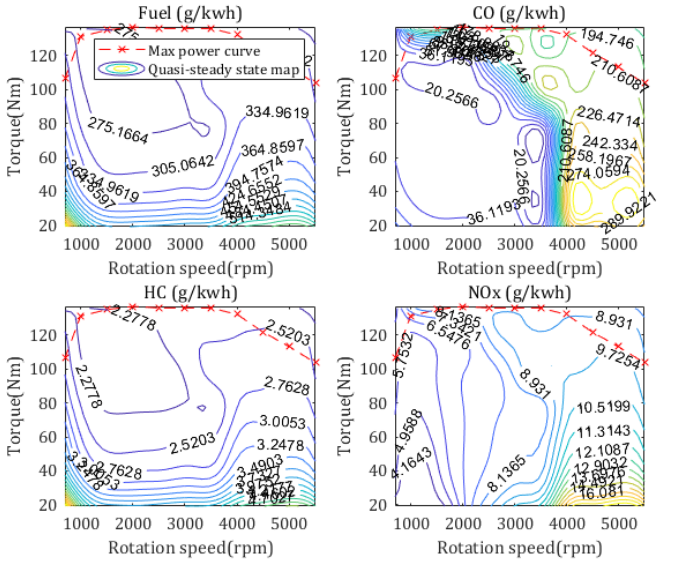

Fig.5. Quasi-steady state cost maps of the studied ICE containing fuel, CO, HC, and NOx [34]

Fig.5 presents quasi-steady state cost maps of a Saturn 1.9 L spark ignition engine with a single overhead camshaft sourced by Argonne National Laboratory, where the maps indicate fuel and studied engine-out emissions that are given in terms of grams per kilowatt hour. Furthermore, the locus of maximum fuel efficiency does not necessarily correspond to the loci of optimum emissions. To reduce fuel consumption and emissions simultaneously, there is a definite trade-off between fuel efficiency and different emissions. Due to different scales of the fuel consumption and emission maps, standardization should be given as

$$\dot{m}_{s,i}(n_{ice}, T_{ice}) = \frac{\dot{m}_i(n_{ice},T_{ice}) - \min[\dot{m}_i(n_{ice},T_{ice})]}{\max[\dot{m}_i(n_{ice},T_{ice})] - \min[\dot{m}_i(n_{ice},T_{ice})]} \quad (9)$$

where $m_i(n_{ice}, T_{ice})$ represents the original cost map, and $\dot{m}_{s,i}(n_{ice}, T_{ice})$ represents the standardized cost map (values are between 0 and 1). After the derivation of the standardized cost map, the weighting process is done by the following equation:

$$\dot{m}_{sw}(n_{ice}, T_{ice}) = \frac{\sum_{i=0}^{i=l} k_i \dot{m}_{s,i}}{\sum_{i=0}^{i=l} k_i} \quad (10)$$

where, the k_i coefficients depend on the components that are demanded to be minimized and the amount of this demand; $i = 1,2,3,4$ corresponding to fuel, CO, HC, and NOx. They are usually a set of fixed values determined by human expertise. However, pedestrians in close proximity to PHEVs optimized by using such cost maps may experience events where CO/HC/NOx concentrations are high enough to cause health effects.

So far, the optimization target combined by introducing the fuzzy adaptive cost map is given by

$$J = \int_0^{t_{end}} \dot{m}_{sw} dt \quad (11)$$

where, t_{end} is the final time stamp of the driving cycle; and $\dot{m}_{sw}$ denotes mass flow rate calculated from the fuzzy adaptive cost map which will be explained in the next section in detail. So far, the constraints will be used in the emission-oriented optimization problem are listed as follows.

$$s.t. \begin{cases} SoC_t, & SoC_t \in [SoC^-, SoC^+] \\ n_{mot,t}, & n_{mot,t} \in [0, n_{mot^*}] \\ T_{mot,t}, & T_{mot,t} \in [-T_{mot^*}, T_{mot^*}] \\ P_{ice,t}, & P_{ice,t} \in [0, P_{ICE^*}] \\ P_{gen,t}, & P_{gen,t} \in [0, -P_{ISG^*}] \end{cases} \quad (12)$$

where, SoC^- and SoC^+ are the lower and upper limits of the value of battery SoC.

B. Fuzzy Satisfying for Pedestrian Adaptation

In order to empower the cost map with an ability to adapt to the density of pedestrians, the relationship between pedestrian density and weights of cost maps needs to be established in reason. Considering the imprecise nature of the decision-maker's judgment, it is natural to assume that the human decision-maker may have fuzzy or imprecise goals for each objective function. Here, fuzzy satisfying approach is developed to interpret the relationship between one input: pedestrian density and four outputs: cost map weights of fuel, CO, HC, and NOx.

The rule base determines the control outputs A, B, C, and D with the inputs state O and P by applying a 'if O and P then A and B and C and D' policy. A mathematical expression of the 'if O then A and B and C and D' policy is

$$[A, B, C, D] = (O \times P) \circ R\,. \quad (13)$$

where, ‘A’, ‘B’, ‘C’, and ‘D’ denote the fuzzy sets of cost map weights related to fuel, CO, HC, and NOx, respectively; ‘O’ denotes the crisp of the reference of scaled pedestrian density, [0,1]; ‘P’ denotes the crisp of the reference of scaled demand power, [0,1]; and ‘R’ denotes the fuzzy relation matrix by cross-product of fuzzy sets of one input.

The original intention of fuzzy rule design is to reduce pedestrian exposure to near-vehicle emissions first and then protect the interest of the car owner. In the input variables, Pedestrian density is a primary factor to measure weights of the weights of emission components (i.e., pedestrian interest) and fuel consumption (i.e., car owner interest). The power demand of the PHEV is a secondary factor that tunes their weight distribution especially for the power demand is extremely low or high. To simplify the expression of $5^2 \times 4 = 100$ fuzzy logic inferences, we assign values to linguistic sets of pedestrian density: ‘very low’ = 1; ‘Low’ = 2; ‘Medium’ = 3; ‘High’ = 4; and ‘very high’ = 5. And to linguistic sets of demand power: ‘very low’ = 5; ‘Low’ = 4; ‘Medium’ = 3; ‘High’ = 2; and ‘very high’ = 1. Therefore, the reasoning process that is based on Eq. (13) with the Sugeno fuzzy set can then be described by the following if-then statements.

$$\left.\begin{matrix} if\ O+P \in [2,3] \\ if\ O+P \in [4,5] \\ if\ O+P \in [6] \\ if\ O+P \in [7,8] \\ if\ O+P \in [9,10] \end{matrix}\right\} then\ A\ is \left\{\begin{matrix} very\ high \\ high \\ medium \\ low \\ very\ low \end{matrix}\right\} and\ B,C,D\ are \left\{\begin{matrix} very\ low \\ low \\ medium \\ high \\ very\ high \end{matrix}\right. \quad (14)$$

In this inference mechanism, the implied fuzzy sets are produced using the max–min composition. In defuzzification, these implied fuzzy sets are combined to provide a crisp value of the controller outputs. There are several approaches [35] to accomplish the defuzzification process, of which the centroid of area method has been chosen for this case. The final output is then measured as the average of the individual centroids weighted by their membership values as follows:

$$Out = \frac{\sum_{i=1}^{n} \pi_i \cdot \varphi_i}{\sum_{i=1}^{n} \varphi_i} \quad , \quad (15)$$

where, π_i is the output of rule base i; φ_i is the centre of the output membership function. Differing the Eq. (10), the weighted summation here refers to the result of the adaptive adjustment of each indicator to the pedestrian density. In this paper, these functions are taken as a typical triangular membership function as follows:

$$q_i = \max\left(\min\left(\frac{x-(0.25i-0.5)}{0.25}, \frac{0.25i-x}{0.25}\right), 0\right), \quad i = 1,2,3,4,5 \quad (16)$$

C. Bees Algorithm for Interactive Optimisation

Due to an addition of external pedestrian information and dynamic optimization objectives, optimization of the pedestrian-aware supervisory control system becomes more difficult. The BA is a swarm-based optimization algorithm created by Pham et al., which follows the natural foraging behavior of honeybees to find an optimal solution [36]. Comparing to the GA and PSO, the BA is more suitable for searching accurately narrow valleys and holes, and for highly multi-modal functions [37], e.g., complex energy management problems. Here, the flowchart of BA-driven interactive optimization with a specific fitness evaluation is shown as Fig. 6, and described as follows:

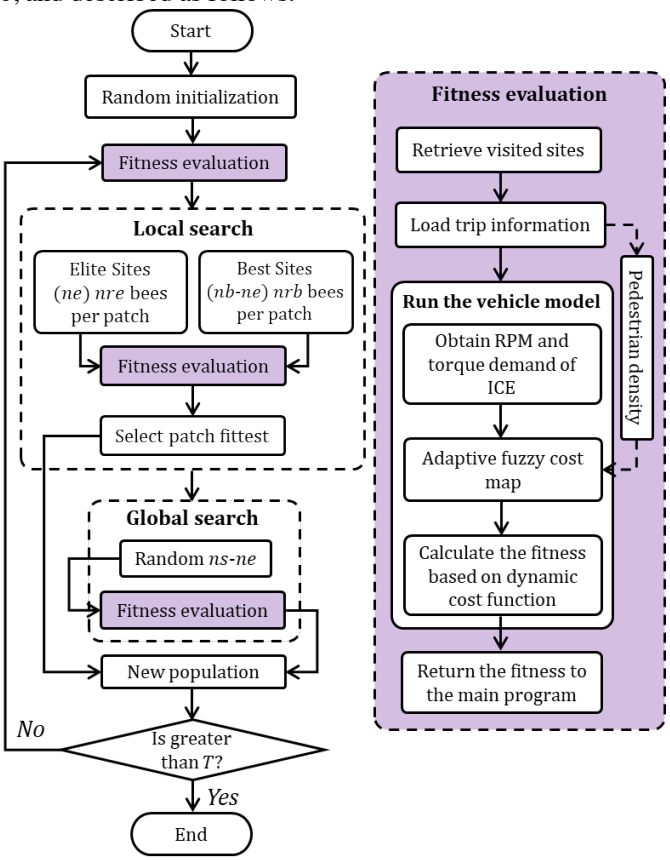

Fig.6. Flowchart of BA-driven interactive optimization

In the BA, each point in the search space (i.e., each potential solution) is regarded as a food source. ‘Scout bees’ randomly collect the space information (i.e., solutions generated randomly). Via the fitness function, ‘Scout bees’ report the quality of the visited locations (i.e., the solutions evaluated). The collected solutions are sorted, and other ‘bees’ are recruited to search the fitness landscape in the neighborhood of the highest-ranking locations (i.e., exploration of other potential solutions close to the best of the generated solutions). The neighborhood of a solution is called a ‘flower patch’. The BA locates the most promising solutions and selectively explores their neighborhoods looking for the global minimum of the objective function (i.e., the solution that minimizes the given cost measure) [37].

Interactive optimization of the pedestrian-aware supervisory control system requires a specific fitness evaluation. Firstly, the visited sites will be retrieved for the fitness evaluation use. Once the PHEV model runs, rpm and torque demand of ICE is acquired. Simultaneously, environmental information about pedestrian density will be loaded to the proposed fuzzy adaptive cost map in order to regulate inter-objective weights of fuel and emissions in a real-time manner. By doing this, the fitness can be calculated and then be returned to the main program.

IV. Experimental Set-up

A. Real-world Cycle Collection

In this section, we present the experimental set-up for the collection of real-world driving cycle information. The testing route that we used in the experiment is exported from the OpenStreetMap and as illustrated in Fig.7.

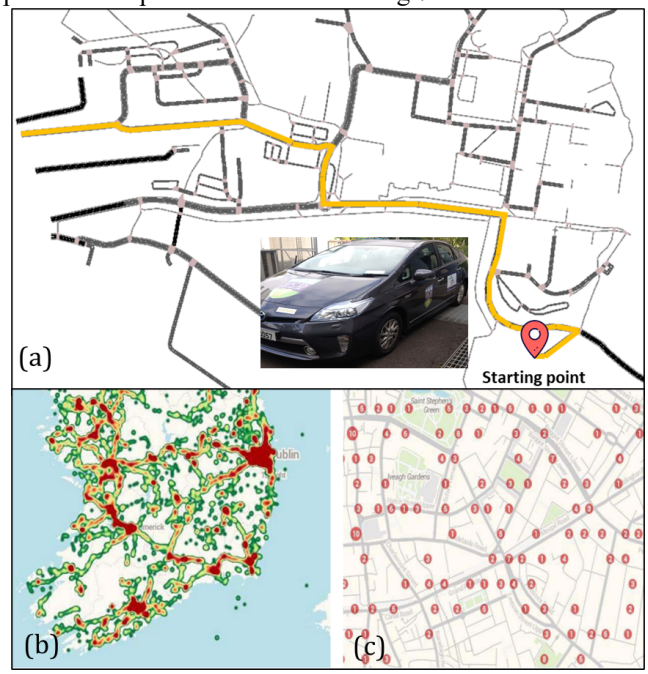

Fig.7. Real-world cycle collection process: a) a testing route in UCD campus; b) a heat map of the density distribution of mobile phone users in Ireland; and c) a cluster map of the density in areas near Dublin city center [19]

As displayed in Fig. 7(a), the route starts from the University College Dublin (UCD) engineering car park and terminates at the western entrance of the UCD campus where it joints the road R825 in Dublin city. The route consists of sidewalks where students, cyclists and local residents can get access from the east to the west of the campus to visit different on-campus facilities. The route is around 1.1km with the speed limit of 35km/h. In a real-world scenario, the route information as such is essentially stored in a vehicle database and can be fetched for analysis when needed. A cloud server is required to act as a central agent being capable of sending specific pedestrian information, via realizable communication channels, to smartphone whenever it receives request. Thus, the real-time density information of pedestrians walking on the sidewalks can be effectively estimated by localization signals from their mobile phones, e.g., GPS, exchanged to the cell towers. Fig. 7(b)(c) displays a heat map of the density distribution of mobile phone users in Ireland (left) and the cluster map of the density in areas near Dublin city center (right) on a typical working day, in which the red area in the heat map specifies higher density than the green area and the number in cluster map specifies the number of signal capacities obtained from the cell towers. Besides, all data is acquired via OpenCellID.org API: http://opencellid.org/api on 5th of July, 2016. Finally, a smartphone (Samsung Galaxy S IV with model no. GT-I9500) is deployed where a specific app based on the Android KitKat operating system is developed and used to collect data transmitted from the vehicle gateway and from the cloud server.

B. Learning Sample Expansion

To investigate the vehicle system robustness improved by the proposed interactive optimization methodology, additional trip information data are required as learning samples to evaluate its behaviors. Since dataset of pedestrian density (as shown in Fig. 6(a)) is small samples from non-normal distributions, resampling techniques can be used to estimate descriptive statistics and confidence intervals from sample data. In our case, Bootstrap (BS) sampling method [38] is adopted that choose random samples with replacement from the sample data to estimate confidence intervals for parameters of interest.

Fig.8 shows the testing driving profiles used in the study including: a) real-world trip information collected with the real-time pedestrian and vehicle speed information; b) real-time pedestrian information resampled; and c) the means and standard deviations of 233 bootstrapped samples. From Fig. 8(b)(c), we can see the distribution of bootstrapped means of random samples is wider than bootstrapped standard deviations of them, which is closer to the distribution range of real data, [0,7] shown in Fig. 8(a). The dataset of pedestrian density resampled by the mentioned two bootstrapped methods then merges with the Worldwide harmonized Light vehicles Test Cycle. The data is used as additional trip samples for the evaluation of vehicle system robustness.

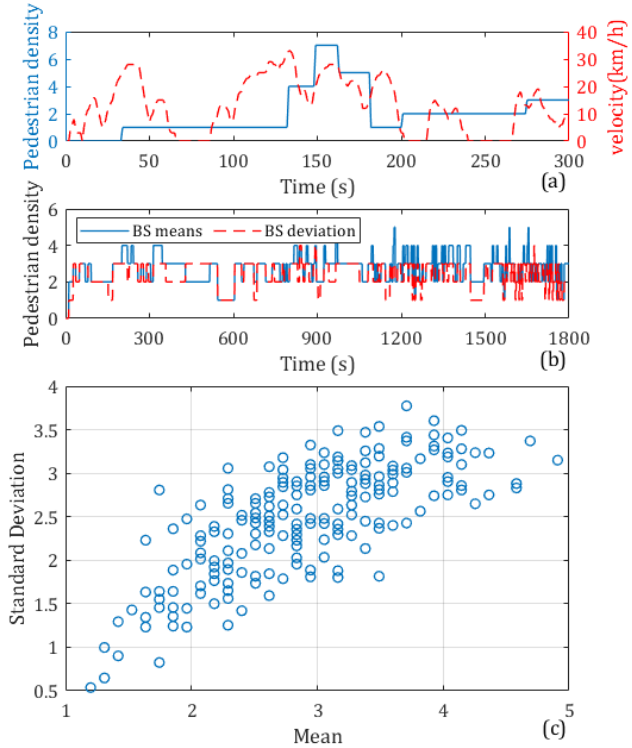

Fig.8. Testing driving profiles including a) real-world trip information collected; b) real-time pedestrian information resampled; and c) 233 estimated pairs of bootstrapped means and standard deviations

V. Results and Discussion

A. Cost Map Adaptability

In this section, the adaptability of the proposed fuzzy adaptive cost map is analyzed, the optimization performance comparisons of three representative algorithms are carried out. Fig.9 displays response surfaces of using the fuzzy satisfying approach. It can be seen that the fuel weight will reach the top

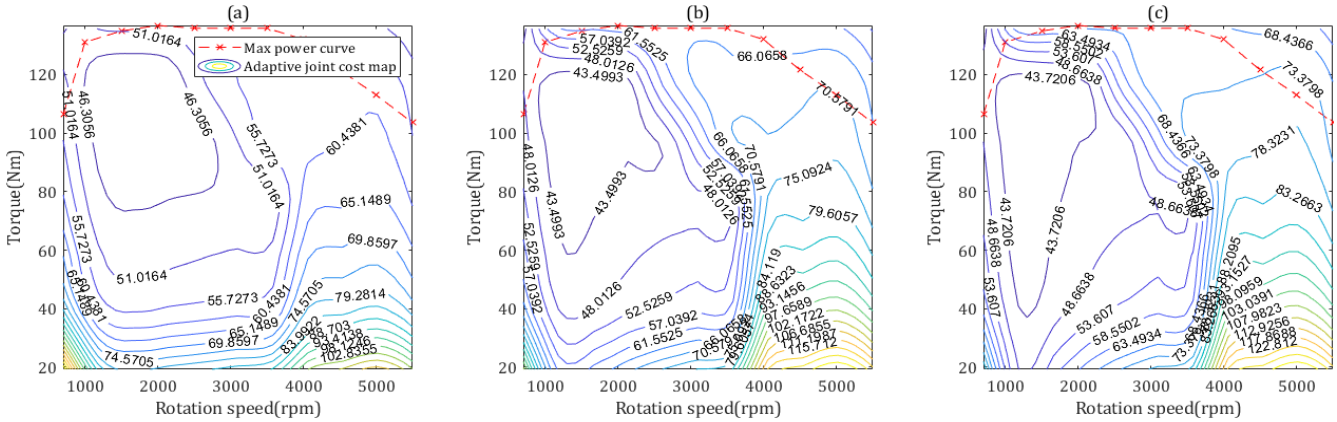

Fig.10. Comparison of the fuzzy adaptive cost map under different pedestrian densities: a) $O = 0$; b) $O = 0.5$; and c) $O = 1$

when whether both pedestrian density and power demand approach to minimum or both approach to maximum. This design is to maximize the interests of car owners when there are few pedestrians or high power requirements. In terms of emissions weight, both pedestrian density and power demand have positive correlation to emissions weight.

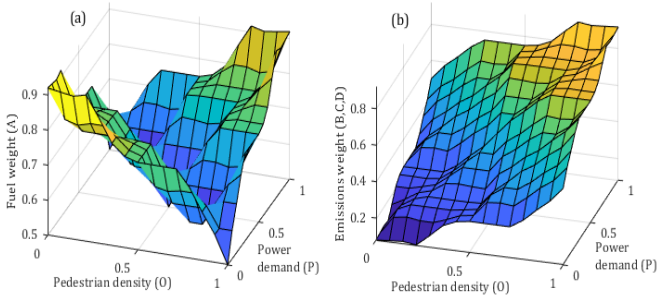

Fig.9. Response surfaces of using the fuzzy satisfying approach for: a) fuel weight; and b) emissions weight

Fig.10 presents the fuzzy adaptive cost map under different pedestrian densities, $O = 0{,}0.5{,}1$. As an increase of pedestrian density, the high-efficiency (peak) area of specific consumption is migrating from the area with $T_{ice} \in [80{,}120], n_{ice} \in [1000{,}2500]$ to the area with $T_{ice} \in [40{,}120], n_{ice} \in [1000{,}2000]$. In conjunction with Fig. 5, because high efficiency area of CO and NOx cost maps occupies the entire low-speed area, the high efficiency area would transfer to this region when pedestrian density increases. But for the area of high speed (> 4000 rpm) and low torque (< 40 Nm) demand, the efficiency is always low. In conjunction with Fig. 9, transition process of weights from fuel to emission components in the fuzzy adaptive cost map is increasing fast first then going to be stable.

B. Interactive Optimization Performance

To evaluate optimization performance of the BA, two representative optimization algorithms of GA and PSO are involved as the baselines. The algorithms were implemented on a laptop with i5-4210H and 8G RAM. Each case runs 30 times on the collected realistic driving cycle repeatedly for twelve rounds and we assume an initial battery SoC of 0.5. For a fair comparison, all optimization algorithms contrast under the same population size, i.e., $N = 20{,}50{,}100$. The termination criterion T is no more than 100 iterations.

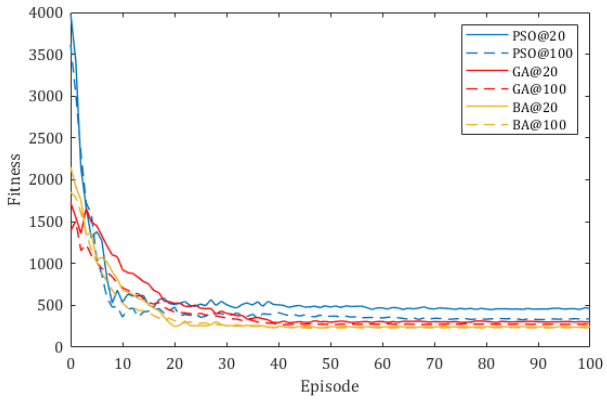

Fig.11. Convergence process of three optimization algorithms during the interactive optimization

Fig.11 illustrates averaged convergence performance of three optimization algorithms during the interactive optimization, where both 20 and 100 population sizes are considered for comparative study. From a view of convergence speed, PSO can fast approach to a stable period (at around 10 iterations) for the interactive optimization compared to BA (at around 15 iterations) and GA (at around 20 iterations). However, PSO has the worst ability to explore the global optimum, which may be due to the simplified particle guidance mechanism. Compared with GA, BA has a faster convergence in the interactive optimization and is more active in exploring the global optimum (at about 15 iterations, its fitness starts to lead). Besides, the optimization performance of PSO is seriously affected by a decrease in population. In general, the BA has superior optimization performance for the pedestrian-aware

supervisory control system interactive optimization compared to other two.

Table II summarizes performance comparison of the studied three optimization algorithms. Here, we define an index of 'success' is that the fitness value of single run cannot be greater than 1% in the value of the best fitness which is achieved by the BA. In terms of the success rate by using three population sizes and three-level iterations, the BA performs entirely significant superiority (198/270) for the interactive optimization contrasted to the other two algorithms. When termination criterion sets to $q = 20$ iterations, the success rate of the BA is nearly twice that of GA, but the PSO has no success to achieve global optimum. For this specific task, the PSO can fast reach an area (Iteration number to 90% success:≤ 12) where potential global peaks emerge but it is extremely hard to detect the global optimum. BA and GA use a more gradual policy (Iteration number to 90% success:≥ 14), in which the population is initially allocated equally into the solution space and is gently made to converge towards the global peak of performance. The convergence process of GA is not easily reversible, and this makes them more prone to becoming trapped by sub-optimal peaks of performance. Moreover, exploitation and exploration in PSO and GA are associated, so their resources should be carefully balanced. This also is the reason why the performance of PSO more sensitive to the choice of an optimal set of learning parameters [37]. Via the interactive optimization, the result of optimal control parameters is listed in Table III.

TABLE II
PERFORMANCE COMPARISON OF THREE OPTIMIZATION ALGORITHMS

Studied algorithm	Population	Iterations to 90% success	Success rate via q iterations		
			q = 20	q = 50	q = 100
GA	20	19	9/30	15/30	16/30
	50	18	11/30	15/30	21/30
	100	14	12/30	19/30	22/30
PSO	20	12	0/30	1/30	0/30
	50	10	0/30	0/30	5/30
	100	10	0/30	2/30	8/30
BA	20	16	14/30	20/30	24/30
	50	16	18/30	21/30	30/30
	100	15	20/30	21/30	30/30

TABLE III
OPTIMIZED RESULT OF THE CONTROL PARAMETERS

Parameter	$\phi_{ice,\alpha}$	$\phi_{ice,\beta}$	$\phi_{gen,\alpha}$	$\phi_{gen,\alpha}$
Value	0.016	0.277	0.360	0.032

As a concept demonstration implemented in real automotive applications, this section shows how to utilize the laboratory cycle (i.e., WLTC) to optimize the pedestrian-aware supervisory control system during real-world driving. The result is based on the studied theoretical vehicle model, but the proposed optimization methodology can be generalized to other cases including actual vehicle control systems.

TABLE V
VEHICLE SYSTEM PERFORMANCE COMPARISON OF USING STUDIED MAPPING TREATMENTS

Mapping treatment	Fuel (g)	SoC	CO production (g)		HC production (g)		NOx production (g)		Total emissions (g)	
			CO mass	Rel. CO mass	HC mass	Rel. HC mass	NOx mass	Rel. NOx mass	Rel. mass	Decline %
Fuel only	880.4	0.232	1.411	0.562	0.827	0.400	0.183	0.099	1.061	-
Equalization	884.4	0.221	1.398	0.584	0.826	0.328	0.188	0.086	0.996	6.13%
CO first	883.6	0.218	1.043	0.496	0.841	0.365	0.174	0.072	0.932	12.16%
FACM	881.2	0.236	1.141	0.529	0.827	0.310	0.183	0.069	0.908	14.42%

C. Vehicle System Economy and Robustness

This section discusses the economy and robustness of the pedestrian-aware supervisory control system using the proposed interactive optimization methodology. Three existing mapping treatments, namely 'Fuel only', 'Equalization' [39] and 'CO first' [40], considered as control groups are summarized in Table IV.

In order to quantify the impact of exhaust emission on the vehicle near the pedestrian, the relative emission mass is defined to evaluate behaviors of three mapping treatments plus one without treatment, which is given as

$$\begin{cases} m'_{i,t} = (1-\eta_i)\int_0^t \dot{m}'_{i,t}dt \\ \dot{m}'_{i,t} = \dot{m}_{i,t} \cdot O \end{cases} \quad (17)$$

where η_i is catalyst removal efficiency for HC, CO and NOx; $\dot{m}'_{i,t}$ and $\dot{m}_{i,t}$ are relative and absolute mass rate of the pollutant i; and O is a real-time signal of scaled pedestrian density, $[0,1]$. In general, catalyst removal efficiency $\eta_i(T_{cat}, \lambda)$ is a function of catalyst temperature T_{cat} and air-fuel ratio λ. Since the purpose of this article is to demonstrate the feasibility and possible benefits of the proposed optimization methodology, high fidelity models of fuel economy and emissions are not the core of this article. Here, the ratio catalyst removal efficiency is considered under an ideal constant scenario with $T_{cat} = 400℃, \lambda = 1$. Here, the catalyst removal efficiency for CO, HC, and NOx is adopted from our previous work [41] is 88%, 98%, 94% respectively.

TABLE IV
INTER-OBJECTIVE WEIGHT COMPARISON OF STUDIED MAPPING TREATMENTS

Mapping treatment	Weight distribution [Fuel CO HC NOx]
Fuel only	[1 0 0 0]
Equalization	[0.25 0.25 0.25 0.25]
CO first	[0.11 0.67 0.11 0.11]
FACM*	Self-adaptive

*Note: 'FACM' indicates fuzzy adaptive cost map.

Table V organizes vehicle system performance comparison of using studied mapping treatments under the realistic driving cycle collected for twelve rounds with an initial battery SoC of 0.5. Only considering fuel consumption in mapping treatment performs the lowest fuel consumption but the highest relative mass of total emissions, compared to the other three. That

means the pedestrians in the testing route expose in the high concentration of CO, HC, and NOx pollutions produced by the studied PHEV. The vehicle system optimized by using the proposed fuzzy adaptive cost map has second rank of fuel used, but the highest value of SoC (0.236). More importantly, for an aspect of avoiding pedestrian expose in near-vehicle emissions, this vehicle system can reduce the total emissions of 14.42%, compared to the two of Equalization (6.13%) and CO first (12.16%). This is attributed to self-regulate inter-objective weights of fuel and exhaust emissions based on a real-time signal of pedestrian density during the optimization process.

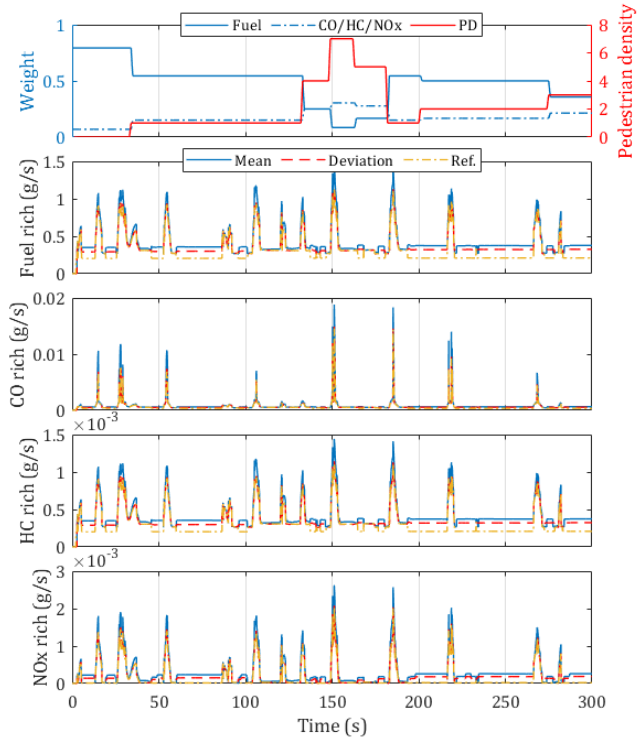

Fig.12. Real-time performance comparison of using two resampling techniques

Fig.12 shows real-time performance comparison over two resampling techniques including bootstrapped means and standard deviations. To better display the details, we intercept one complete cycle [0,300] as a representative for analysis. From the results, the weights for exhaust emissions are increasing and the weight of fuel consumption is reducing when the vehicle reaches the area with higher pedestrian density. Comparing to using the bootstrapped mean technique, the PHEV system optimized by using standard deviation technique shows stronger adaptability to the testing cycle that saves more fuel and reduce more exhaust emissions. In conjunction with Fig. 5, the bootstrapped deviation technique uses conservative policy to assign random samples to a higher probability interval. Relatively, the bootstrapped mean technique intends to restore distribution of original samples as much as possible, however, several marginal samples occur, which cannot be aligned with the timing of other information in the original sample.

In Fig. 13, the overall performance of the vehicle system optimized by two resampling techniques including bootstrapped means and standard deviations is further compared. As expected, the vehicle system optimized by using bootstrapped mean technique performs the worse performance in terms of fuel, CO, HC, and NOx. Although using this technique can acquire the higher value of SoC (0.246), it cannot effectively convert this surplus electricity to a reduction on fuel and emissions. At this point, using the bootstrapped deviation technique make it up for better fuel economy (0.5%) and lower relative emissions (> 1.1%) to the pedestrians, compared to the bootstrapped mean one. In general, the studied two resampling techniques both are alternative solutions for the regeneration of driving cycle-related information, where the deterioration ≤ 5.80%. Compared to using bootstrapped mean technique, the deterioration of using the bootstrapped deviation one can be further reduced to 2.17%.

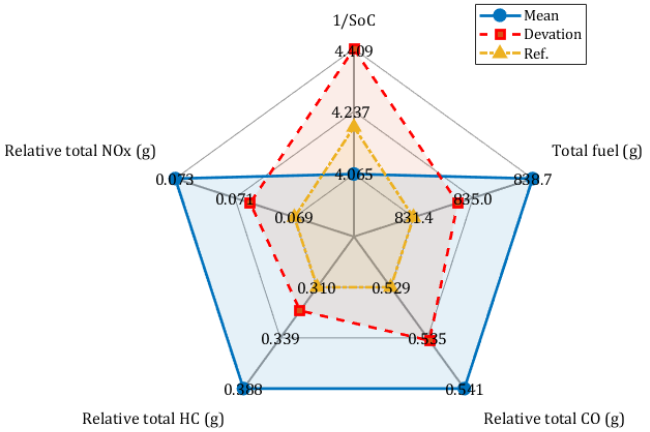

Fig.13. The overall performance comparison improved by using two BS techniques

D. Effect of Communication Quality

Efficient communication is the key to the success of the distributed system. However, signal loss and delay also happen from time to time. For CAVs, the quality of the signal sent and received by the vehicle terminal as a whole has to be seriously considered [42]. As reported in [43], 0-2000 ms is a regular range of latency of dedicated short-range communications and 4G-LTE for connected vehicles. However, the refresh rate of pedestrian density information is not high (every 100 meters), after investigation, it has a little reduction on the fuel-saving performance ($< 0.1\%$) even if the communication delay reaches 2000ms. In view of this, this section discusses the impact of signal loss on the pedestrian-aware supervisory control system.

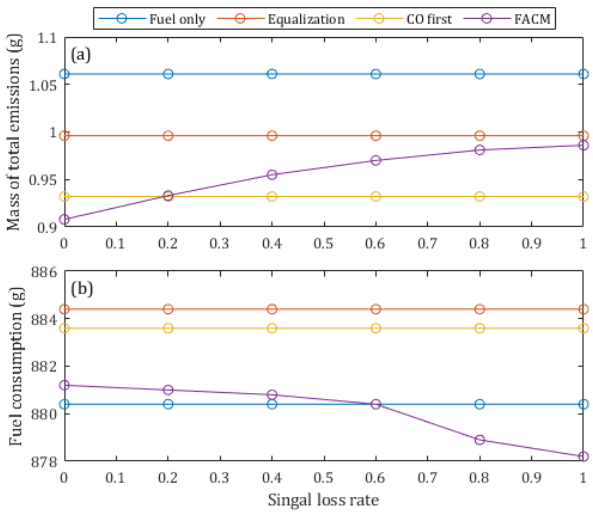

Fig.14. System robustness performance under different signal loss rates

To emulate signal loss of the V2X network between the vehicle and roadside unit, six levels of signal loss rate are considered and were used to investigate the robustness of the proposed pedestrian-aware supervisory control system. A trigger square signal was designed to multiply the original signal, where each trigger segment is used to activate the pedestrian density signal and its duration is fixed at 30 s. Conversely, the non-trigger segment is used to deactivate the pedestrian density signal and its duration is based on the signal loss rate. Obviously, the 'Fuel only', 'Equalization', and 'CO first' treatments are not affected by signal loss because of their fixed weights of fuel and emission components during real-time driving. As signal loss rate increases, the mass of total emissions obtained by pedestrian-aware supervisory control system using the proposed fuzzy adaptive cost map increases gradually. Relatively, the fuel consumption obtained by this system decreases slowly first to at 0.6 of signal lass rate and then drop fast to 878.2 g. When the signal is completely lost, the proposed system (with relative low mass of total emissions and the lowest fuel consumption) still has strong robustness, where the only thing changed is the system benefit has been transited from pedestrians to the car owner.

VI. Conclusion

This paper proposes an interactive optimization methodology for the pedestrian-aware supervisory control system of connected HEVs, which combines a new fuzzy adaptive cost map and the Bees Algorithm to optimize power-split control parameters. The comparative study including mapping treatment methods and optimization algorithm performance as well as economy and robustness of PHEV systems has been carried out. The conclusions drawn from the investigation are as follows:

1) The developed fuzzy adaptive cost map can activate fixed weights of sub-maps and enable the self-regulation of inter-objective weights based on the pedestrian density of the testing scenario.
2) 14.42% mass of exhaust emissions can be reduced for the involved pedestrians with help of the proposed approach, compared to only considering fuel consumption in mapping treatment.
3) The modified BA for the interactive optimization shows the ability to achieve the highest success rate (86/90), which exhibits a superiority in control optimization of connected HEVs, compared to the two baselines: genetic algorithm (79/90) and particle swarm optimization (13/90).
4) The proposed bootstrapped deviation technique makes it up for better fuel economy (0.5%) and lower emissions ($> 1.1\%$) to the pedestrians, compared to the bootstrapped mean one.
5) When the signal is completely lost, the proposed system (with relative low mass of total emissions and the lowest fuel consumption) still has strong robustness, where the only thing changed is the system benefit has been transited from pedestrians to the car owner.

The work presented in this paper is a significant step towards 'pedestrian-aware supervisory control system'. However, it is only a first step and neglects some aspects of a complete solution, and these will be the subject of future work. For instance, the proposed system does not explicitly model the evolution of pollution and realistic dispersion models, as well as the impact of topology. The other uncertainty in the context of electric vehicles is the energy needs of the drivers, and models to capture this uncertainty would be studied in future work.

References

[1] S. M. Shiva Nagendra, U. Schlink, V. Dheeraj Alshetty, M. Diya, and J. S. Menon, *Traffic-related air pollution, human exposure, and commercially available market solutions: Perspectives from the developing nation context*, no. iii. Elsevier Inc., 2020. doi: 10.1016/b978-0-12-818122-5.00022-3.

[2] H. Khreis, C. Kelly, J. Tate, R. Parslow, K. Lucas, and M. Nieuwenhuijsen, "Exposure to traffic-related air pollution and risk of development of childhood asthma: A systematic review and meta-analysis," *Environment International*, vol. 100, pp. 1–31, 2017, doi: 10.1016/j.envint.2016.11.012.

[3] J. Naoum-Sawaya, E. Crisostomi, M. Liu, Y. Gu, and R. Shorten, "Smart Procurement of Naturally Generated Energy (SPONGE) for Plug-In Hybrid Electric Buses," *IEEE Transactions on Automation Science and Engineering*, vol. 14, no. 2, pp. 598–607, 2017, doi: 10.1109/TASE.2016.2633001.

[4] J. Li, D. Wu, H. Mohammadsami Attar, and H. Xu, "Geometric neuro-fuzzy transfer learning for in-cylinder pressure modelling of a diesel engine fuelled with raw microalgae oil," *Applied Energy*, vol. 306, p. 118014, Jan. 2022, doi: 10.1016/j.apenergy.2021.118014.

[5] Q. Zhou *et al.*, "Multi-step Reinforcement Learning for Model-Free Predictive Energy Management of an Electrified Off-highway Vehicle," *Applied Energy*, vol. 255, no. 2019, pp. 588–601, 2019.

[6] C. Yang, M. Zha, W. Wang, K. Liu, and C. Xiang, "Efficient energy management strategy for hybrid electric vehicles/plug-in hybrid electric vehicles: Review and recent advances under intelligent transportation system," *IET Intelligent Transport Systems*, vol. 14, no. 7, pp. 702–711, 2020, doi: 10.1049/iet-its.2019.0606.

[7] Y. Huang, H. Wang, A. Khajepour, H. He, and J. Ji, "Model predictive control power management strategies for HEVs : A review," *Journal of Power Sources*, vol. 341, pp. 91–106, 2017, doi: 10.1016/j.jpowsour.2016.11.106.

[8] W. Enang and C. Bannister, "Modelling and control of hybrid electric vehicles (A comprehensive review)," *Renewable and Sustainable Energy Reviews*, vol. 74, no. March, pp. 1210–1239, 2017, doi: 10.1016/j.rser.2017.01.075.

[9] J. Li, Q. Zhou, H. Williams, H. Xu, and C. Du, "Cyber-Physical Data Fusion in Surrogate-assisted Strength Pareto Evolutionary Algorithm for PHEV Energy Management Optimization," *IEEE Transactions on Industrial Informatics*, pp. 1–1, 2021, doi: 10.1109/TII.2021.3121287.

[10] Q. Zhou, D. Zhao, B. Shuai, Y. Li, H. Williams, and H. Xu, "Knowledge Implementation and Transfer With an Adaptive Learning Network for Real-Time Power Management of the Plug-in Hybrid Vehicle," *IEEE Transactions on Neural Networks and Learning Systems*, vol. PP, pp. 1–11, 2021, doi: 10.1109/TNNLS.2021.3093429.

[11] Q. Zhou *et al.*, "Transferable Representation Modelling for Real-time Energy Management of the Plug-in Hybrid Vehicle based on K-fold Fuzzy Learning and Gaussian Process Regression," *Applied Energy*, 2021.

[12] M. Montazeri-Gh, A. Poursamad, and B. Ghalichi, "Application of genetic algorithm for optimization of control strategy in parallel hybrid electric vehicles," *Metal Finishing*, vol. 104, no. 6, pp. 420–435, 2006, doi: 10.1016/j.jfranklin.2006.02.015.

[13] J. Li, Q. Zhou, H. Williams, and H. Xu, "Back-to-back competitive learning mechanism for fuzzy logic based supervisory control system of hybrid electric vehicles," *IEEE Transactions on Industrial Electronics*, vol. 67, no. 10, pp. 8900–8909, 2020, doi: 10.1109/TIE.2019.2946571.

[14] J. Li *et al.*, "Dual-loop online intelligent programming for driver-oriented predict energy management of plug-in hybrid electric vehicles," *Applied Energy*, vol. 253, no. November, p. 113617, 2019, doi: 10.1016/j.apenergy.2019.113617.

[15] D. T. Pham and M. Castellani, "A comparative study of the Bees Algorithm as a tool for function optimisation," *Cogent Engineering*, vol. 2, no. 1, pp. 1–28, 2015, doi: 10.1080/23311916.2015.1091540.

[16] L. Zhang, Z. Zhang, Z. Wang, J. Deng, and D. G. Dorrell, "Chassis Coordinated Control for Full X-by-Wire Vehicles-A Review," *Chinese Journal of Mechanical Engineering (English Edition)*, vol. 34, no. 1. Springer, Dec. 01, 2021. doi: 10.1186/s10033-021-00555-6.

[17] A. Rezaei, J. B. Burl, B. Zhou, and M. Rezaei, "A New Real-Time Optimal Energy Management Strategy for Parallel Hybrid Electric Vehicles," *IEEE Transactions on Control Systems Technology*, vol. 27, no. 2, pp. 830–837, 2019, doi: 10.1109/TCST.2017.2775184.

[18] X. Qi, Y. Luo, G. Wu, K. Boriboonsomsin, and M. Barth, "Deep reinforcement learning enabled self-learning control for energy efficient driving," *Transportation Research Part C: Emerging Technologies*, vol. 99, no. December 2018, pp. 67–81, 2019, doi: 10.1016/j.trc.2018.12.018.

[19] Y. Gu, M. Liu, J. Naoum-sawaya, E. Crisostomi, G. Russo, and R. Shorten, "Pedestrian-Aware Engine Management Strategies for Plug-In Hybrid Electric Vehicles," vol. 19, no. 1, pp. 92–101, 2018.

[20] S. Bahrami, M. Nourinejad, G. Amirjamshidi, and M. J. Roorda, "The Plugin Hybrid Electric Vehicle routing problem: A power-management strategy model," *Transportation Research Part C: Emerging Technologies*, vol. 111, no. May 2017, pp. 318–333, 2020, doi: 10.1016/j.trc.2019.12.006.

[21] P. Kopelias, E. Demiridi, K. Vogiatzis, A. Skabardonis, and V. Zafiropoulou, "Connected & autonomous vehicles – Environmental impacts – A review," *Science of the Total Environment*, vol. 712, p. 135237, 2020, doi: 10.1016/j.scitotenv.2019.135237.

[22] C. Huang, R. Salehi, T. Ersal, and A. G. Stefanopoulou, "An energy and emission conscious adaptive cruise controller for a connected automated diesel truck," *Vehicle System Dynamics*, vol. 58, no. 5, pp. 805–825, 2020, doi: 10.1080/00423114.2020.1740283.

[23] Y. Shao and Z. Sun, "Vehicle Speed and Gear Position Co-Optimization for Energy-Efficient Connected and Autonomous Vehicles," *IEEE Transactions on Control Systems Technology*, vol. 29, no. 4, pp. 1721–1732, 2020.

[24] A. Vahidi and A. Sciarretta, "Energy saving potentials of connected and automated vehicles," *Transportation Research Part C: Emerging Technologies*, vol. 95, no. September 2018, pp. 822–843, 2018, doi: 10.1016/j.trc.2018.09.001.

[25] S. E. Li and Y. Zheng, "Dynamical Modeling and Distributed Control of Connected and Automated Vehicles: Challenges and Opportunities," *IEEE Intelligent Transportation Systems Magazine*, vol. 9, pp. 46–58, 2017.

[26] L. Zhang, Z. Wang, X. Ding, S. Li, and Z. Wang, "Fault-Tolerant Control for Intelligent Electrified Vehicles against Front Wheel Steering Angle Sensor Faults during Trajectory Tracking," *IEEE Access*, vol. 9, pp. 65174–65186, 2021, doi: 10.1109/ACCESS.2021.3075325.

[27] M. Ehsani, Y. Gao, S. Longo, and K. Ebrahimi, *Modern electric, hybrid electric, and fuel cell vehicles*. CRC press, 2018.

[28] J. Li, Q. Zhou, Y. He, H. Williams, and H. Xu, "Driver-identified Supervisory Control System of Hybrid Electric Vehicles based on Spectrum-guided Fuzzy Feature Extraction," *IEEE Transactions on Fuzzy Systems*, vol. 6706, no. c, pp. 1–1, 2020, doi: 10.1109/tfuzz.2020.2972843.

[29] Q. Zhou, Y. Zhang, Z. Li, J. Li, H. Xu, and O. Olatunbosun, "Cyber-Physical Energy-Saving Control for Hybrid Aircraft-Towing Tractor Based on Online Swarm Intelligent Programming," *IEEE TRANSACTIONS ON INDUSTRIAL INFORMATICS*, vol. 14, no. 9, pp. 4149–4158, 2018, doi: 10.1109/TII.2017.2781230.

[30] J. Peng, H. He, and R. Xiong, "Rule based energy management strategy for a series – parallel plug-in hybrid electric bus optimized by dynamic programming," *Applied Energy*, vol. 185, pp. 1633–1643, 2017, doi: 10.1016/j.apenergy.2015.12.031.

[31] Z. Chen, R. Xiong, C. Wang, and J. Cao, "An on-line predictive energy management strategy for plug-in hybrid electric vehicles to counter the uncertain prediction of the driving cycle," *Applied Energy*, vol. 185, pp. 1663–1672, 2017, doi: 10.1016/j.apenergy.2016.01.071.

[32] M. Deb, B. Debbarma, A. Majumder, and R. Banerjee, "Performance –emission optimization of a diesel-hydrogen dual fuel operation: A NSGA II coupled TOPSIS MADM approach," *Energy*, vol. 117, pp. 281–290, 2016, doi: 10.1016/j.energy.2016.10.088.

[33] P. Michel, A. Charlet, G. Colin, Y. Chamaillard, G. Bloch, and C. Nouillant, "Optimizing fuel consumption and pollutant emissions of gasoline-HEV with catalytic converter," *Control Engineering Practice*, vol. 61, pp. 198–205, 2017, doi: 10.1016/j.conengprac.2015.12.010.

[34] A. Brooker *et al.*, "ADVISOR Advanced Vehicle Simulator," *National Renewable Energy Laboratory*, 2013. http://adv-vehicle-sim.sourceforge.net/

[35] L. A. H. Zad, "A fuzzy-algorithmic approach to the definition of complex or imprecise concepts," *International Journal of Man-Machine Studies*, pp. 249–291, 1976.

[36] D. T. Pham, A. Ghanbarzadeh, E. Koç, S. Otri, S. Rahim, and M. Zaidi, "The Bees Algorithm - A Novel Tool for Complex Optimisation Problems," *Intelligent Production Machines and Systems - 2nd I*PROMS Virtual International Conference 3-14 July 2006*, pp. 454–459, 2006, doi: 10.1016/B978-008045157-2/50081-X.

[37] D. T. Pham and M. Castellani, "The bees algorithm: Modelling foraging behaviour to solve continuous optimization problems," *Proceedings of the Institution of Mechanical Engineers, Part C: Journal of Mechanical Engineering Science*, vol. 223, no. 12, pp. 2919–2938, 2009, doi: 10.1243/09544062JMES1494.

[38] B. Efron and R. J. Tibshirani, *An introduction to the bootstrap*. 1994.

[39] V. Sezer, M. Gokasan, and S. Bogosyan, "A novel ECMS and combined cost map approach for high-efficiency series hybrid electric vehicles," *IEEE Transactions on Vehicular Technology*, vol. 60, no. 8, pp. 3557–3570, 2011, doi: 10.1109/TVT.2011.2166981.

[40] Y. Wang, Y. Shen, X. Yuan, and Y. Yang, "Operating point optimization of auxiliary power unit based on dynamic combined cost map and particle swarm optimization," *IEEE Transactions on Power Electronics*, vol. 30, no. 12, pp. 7038–7050, 2015, doi: 10.1109/TPEL.2014.2383443.

[41] A. O. Hasan, A. Abu-Jrai, A. H. Al-Muhtaseb, A. Tsolakis, and H. Xu, "HC, CO and NOx emissions reduction efficiency of a prototype catalyst in gasoline bi-mode SI/HCCI engine," *Journal of Environmental Chemical Engineering*, vol. 4, no. 2, pp. 2410–2416, 2016, doi: 10.1016/j.jece.2016.04.015.

[42] J. He, K. Yang, and H. H. Chen, "6G Cellular Networks and Connected Autonomous Vehicles," *IEEE Network*, vol. 35, no. 4, pp. 255–261, Jul. 2021, doi: 10.1109/MNET.011.2000541.

[43] K. C. Dey, A. Rayamajhi, M. Chowdhury, P. Bhavsar, and J. Martin, "Vehicle-to-vehicle (V2V) and vehicle-to-infrastructure (V2I) communication in a heterogeneous wireless network - Performance evaluation," *Transportation Research Part C: Emerging Technologies*, vol. 68, pp. 168–184, 2016, doi: 10.1016/j.trc.2016.03.008.

Ji Li (M'19) awarded the Ph.D. degree in mechanical engineering from the University of Birmingham (UoB), U.K, in 2020. He is currently a Research Fellow and works on the Connected and Autonomous Systems for Electrified Vehicles at the Vehicle Technology Research Centre. His current research interests include computational intelligence, informatic fusion, data-driven modelling, man-machine system, and their applications on connected and autonomous vehicles.

Yingqi Gu (M'17) received the Ph.D. degree in Control Engineering and Decision Science from School of Electrical and Electronic Engineering, University College Dublin. She currently is a postdoc research fellow with the Insight Centre for Data Analytics at Dublin City University, and an adjunct lecturer at National University of Ireland Maynooth. Her current research interests include AI & machine learning, control and optimization theories with applications to electric vehicles, intelligent transportation systems, and smart healthcare systems.

Chongming Wang received the Ph.D. in Mechanical Engineering from Vehicle and Engine Technology Research Centre, University of Birmingham, Birmingham, UK. His PhD thesis was about engine performance and emissions of various advanced biofuel candidates. Currently, he is an assistant professor at the Centre for Advanced Low Carbon Propulsion Systems (C-ALPS), Coventry University, Coventry, U.K. His research is mainly focusing on health and safety of lithium-ion batteries, or more specifically, battery ageing and thermal management.

Mingming Liu (M'15) received the Ph.D. degree from the Hamilton Institute, Maynooth University in 2015. After that, he worked at University College Dublin as a senior postdoctoral researcher and then at IBM Ireland Lab as a data scientist, applied researcher, and H2020 project lead. He is currently working as an Assistant Professor in the School of Electronic Engineering at Dublin City University. His research interests include control and optimization theories with applications to 5G & IoT, electric vehicles, smart grids, intelligent transportation systems and smart cities.

Quan Zhou (M'17) received the Ph.D. degree in mechanical engineering from the University of Birmingham in 2019 that was distinguished by being the school's solo recipient of the University of Birmingham's Ratcliffe Prize of the year. He is currently a Research Fellow and leads the Connected and Autonomous Systems for Electrified Vehicles Research at University of Birmingham. His research interests include evolutionary computation, fuzzy logic, reinforcement learning, and their application in vehicular systems.

Guoxiang Lu received the Ph.D. degree in control engineering in 2010. He started a research fellow and led the development of modern engine control at the UoB, U.K., in 2015. He is currently senior manager at department of research and development of renewable and sustainable vehicles, BYD Auto Ltd, Guangzhou, China. His research interests include GDI engine combustion control, system modeling, real-time control, engine control strategy development, and intelligent vehicle system.

Duc Truong Pham received the Ph.D. degree in mechanical engineering from the University of Birmingham, Birmingham, U.K., in 1992. He is currently a Professor with the School of Mechanical Engineering, University of Birmingham, U.K. He is a Fellow of the Royal Academy of Engineering, the Learned Society of Wales, the Society of Manufacturing Engineers, the Institution of Engineering and Technology, and the Institution of Mechanical Engineers. His academic output includes more than 500 technical papers and 15 books. He has supervised over 100 PhD theses to completion. He has won in excess of £30M in external research grants and contracts.

Hongming Xu received the Ph.D. degree in mechanical engineering from Imperial College London, London, U.K. He is a Professor of Energy and Automotive Engineering at the University of Birmingham, Birmingham, U.K., and Head of Vehicle and Engine Technology Research Centre. He has six years of industrial experience with Jaguar Land Rover. He has authored and co-authored more than 400 journal and conference publications on advanced vehicle powertrain systems involving both experimental and modeling studies.